

DEER Sensitivity Between Iron Centers and Nitroxides in Heme-containing Proteins Improves Dramatically Using Broadband, High-field EPR

Claire L. Motion[†], Janet E. Lovett[†], Stacey Bell[†], Scott L. Cassidy[†], Paul A. S. Cruickshank[†], David R. Bolton[†], Robert I. Hunter[†], Hassane El Mkami[†], Sabine Van Doorslaer[‡] and Graham M. Smith^{†,}.*

[†]SUPA, School of Physics & Astronomy, University of St Andrews, KY16 9SS

[‡]Department of Physics, University of Antwerp, Antwerp, Belgium.

Contents

Sample preparation
EPR Spectroscopy
DEER results and MMM simulation
Composite pulses and sequences used
 T_1 and T_m measurements
Signal-to-noise analysis.
Q-band DEER

Sample preparation

Human neuroglobin C120R1: Protein mutagenesis, purification and spin labelling was performed as described in ref¹. An MTSL (1-oxy-2,2,5,5-tetramethylpyrroline-3-methyl) nitroxide spin label was attached at Cys120 of a Cys46Ser/Cys55Ser mutant of human neuroglobin. This mutant is referred to as NGB-C120R1 in the text. Its concentration was 1.1 mM heme content.

Metmyoglobin mutants

The sperm whale myoglobin expression plasmids were originally supplied by Professor Jason Chin, MRC, Cambridge². They contain an C-terminal HisTag.

Forward primers used in mutagenesis from the wildtype sequence are:

S3C accatggttctgtgtgaaggtgaatgg

S117C catgttctgcattgtagacatccagg

Mutagenesis was carried out using the Quikchange Site-Directed Mutagenesis Kit (Stratagene) following the manufacturer's instructions.

The protein was expressed in *Escherichia coli* strain DH10 β using Luria-Bertani broth with kanamycin and tetracycline antibiotics. Cultures were incubated at 37°C until an optical density of 0.6-0.8 was reached. Expression was induced using L-arabinose (0.2% weight/volume final concentration) and cells were left at 37°C for a further 5 hours.

Cells were lysed using sonication. Immediately following lysis a final concentration of 50 mM DTT was added. Protein was purified using a 5ml Ni₂-NTA Superflow Cartridge (QIAGEN) following dilution. The protein was removed from the column in 50 mM HEPES, 125mM NaCl and 0.5M imidazole, pH 7.0. This was treated with 10 mM DTT and further purified using size exclusion chromatography with a HiLoad 16/600 Superdex S-75 column (GEHealthcare) into 50 mM HEPES, 125 mM NaCl, pH 7.0. An SDS-PAGE gel with coomassie staining was used to confirm the purity of the monomeric species. A greater than 5 times excess of MTS spin label (Toronto Research Chemicals) was added and the protein was left at room temperature for about 1 hour. The protein was transferred into 50 mM HEPES, 125 mM NaCl, 200 mM imidazole, pH 7.0 buffer in deuterium oxide using a centrifuge concentrator with 10KDa molecular weight cut-off. Spin-labeling efficiency was estimated to be 100% through comparisons with other labeled proteins and TEMPO standards. Uv-vis absorption data was collected to assess protein

concentration and the nature of the heme iron. The extinction coefficient at 280nm was estimated to be $15,470 \text{ M}^{-1}\text{cm}^{-1}$ by ExPASy³ for apo-Myo and we used $31,500 \text{ M}^{-1}\text{cm}^{-1}$ from the data available in Reference⁴ for met-Myo. The remaining absorption spectrum closely resembled that reported for hydroxyl bound, low spin, metmyoglobin⁴ with peaks at approximately 415, 540 and 580 nm. The spectra differed for the S3C, S117C and S3CS117C mutants with the S3C resembling the hydroxyl bound metmyoglobin absorption profile the most, and the two samples with S117C mutation looking similar. Both forms showed incomplete heme binding with, assuming the hydroxyl-met-Myo extinction coefficients in Reference⁴, approximately 70% heme occupancy for the S117C, 95% for S3CS117C and 100% for S3C.

EPR spectroscopy

Sample preparation

NGB: C120R1 protein solutions (pH 8.5) were mixed 1:1 with glycerol leading to final concentration of 1.1 mM (heme content) and then flash frozen in FEP sample tubes using liquid nitrogen before cold loading into the spectrometer at 140 K. The sample was then annealed by raising the temperature of the cryostat gradually to 180 K for a short time, before measurements were made at 6 K. Annealing is carried out to remove any cracks in the sample that may occur during the flash-freezing process.

Metmyoglobin: 50 μl of the final protein solution had 50 μl deuterated glycerol (CK Isotopes) by volume added. The final concentrations of the samples were: Mb-S3CR1: 0.18 mM, Mb-S117R1: 0.2 mM and Mb-S3R1S117R1: 0.14 mM. Samples were loaded into FEP sample tubes and flash frozen using liquid nitrogen and stored at this temperature until measurement. The samples were also loaded at 140 K, and were annealed similarly to the NGB case before being lowered to measurement temperature of 6 or 58 K.

Pulsed EPR

All W-band experiments were carried out at 94 GHz on a home built high power pulsed spectrometer (HiPER⁵) incorporating a continuous flow helium cryostat (CF935) and a temperature control system (ITC 502) from Oxford instruments. Experiments on NGB, Mb-

S3R1, Mb-S117R1 and Mb-S3R1S117R1 (Fe(III)-nitroxide measurement) were conducted at 6 K and on Mb-S3R1S117R1 (nitroxide-nitroxide measurement) at 58 K.

Field swept echo: experiment was carried out using the $\pi/2 - \tau - \pi - \tau - echo$ sequence with pulse lengths $t_{\pi/2} = 6$ ns and $t_{\pi} = 12$ ns, and inter-pulse delay of 1000 ns. The refocused echo experiments were carried out using the $\pi/2 - \tau_1 - \pi - (\tau_1 + \tau_2) - \pi - \tau_2 - echo$ sequence with pulse lengths $t_{\pi/2} = 8$ ns and $t_{\pi} = 16$ ns for standard pulses and $t_{\pi\text{composite}} = 8+16+24$ ns for composite pulses, and inter-pulse delays of $\tau_1=198$ ns and $\tau_2 = 954$ ns.

DEER experiments on NGB were carried out using the four-pulse sequence (Figure 1), $\pi/2(f_{\text{obs}}) - \tau_1 - \pi(f_{\text{obs}}) - (\tau_1+t) - \pi(f_{\text{pump}}) - (\tau_2-t) - \pi(f_{\text{obs}}) - \tau_2 - echo$, with pulse lengths $t_{\pi/2} = 8$ ns and $t_{\pi} = 16$ ns for standard pulses and $t_{\pi\text{composite}} = 8+16+24$ ns for composite pulses and $\tau_1=198$ ns and $\tau_2 = 954$ ns. The pump pulse started 100 ns after the first π pulse on the observer sequence, and was incremented in 4 ns steps for 201 steps. Observer pulse frequency was 93.9996 GHz and the pump frequency was 93.68604 GHz, giving a frequency offset of 313.56 MHz. Sequence repetition frequency was 1 kHz with 1 second per point averaging. This was averaged for 9 scans, taking ~30 minutes to complete for each data set using the 4 composite DEER combinations.

Mb-S3R1 inter-pulse delays were $\tau_1=198$ ns and $\tau_2 = 1454$ ns, with the same pulse lengths as for NGB. The pump pulse was started 100 ns after the first π pulse on the observer sequence and was incremented in 8 ns steps for 182 steps. Observer pulse frequency was 93.9996 GHz and the pump frequency was 93.64956 GHz, giving a frequency offset of 350 MHz. This was averaged at 10 kHz for 12 scans taking approximately 37 minutes to run.

Mb-S117R1 inter-pulse delays were $\tau_1=244$ ns and $\tau_2 = 964$ ns, with the same pulse lengths as for NGB. τ_1 was optimised to minimize the effect of ESEEM. The pump pulse was started 156 ns after the first π pulse on the observer sequence and was incremented in 8 ns steps for 124 steps. Observer pulse frequency was 93.9996 GHz and the pump frequency was 93.64956 GHz, giving a frequency offset of 350 MHz. This was averaged at 10 kHz for 9 scans taking approximately 19 minutes to run.

Mb-S3R1S117R1 inter-pulse delays were $\tau_1 = 226$ ns and $\tau_2 = 1498$ ns, with the same pulse lengths as for NGB. The pump pulse was started 124 ns after the first π pulse on the observer

sequence and was incremented in 8 ns steps for 187 steps. Observer pulse frequency was 93.9996 GHz and the pump frequency was 93.64956 GHz, giving a frequency offset of 350 MHz. This was averaged at 10 kHz for 12 scans taking approximately 38 minutes to run.

S3R1-S117R1 inter-pulse delays were $\tau_1=260$ ns and $\tau_2 = 1990$ ns, with all standard pulses with pulse lengths $t_{\pi/2} = 6$ ns and $t_{\pi} = 12$ ns. The pump pulse was started 100 ns after the first π pulse on the observer sequence and was incremented in 8 ns steps for 262 steps. Frequency of observer pulse was 93.78516 GHz (g_z) and the pump pulse was 93.92004 GHz (g_y), giving a frequency offset of 134 MHz. This was averaged at 1 kHz for a single scan, which took approximately 5 minutes to run.

All DEER traces were then processed using DeerAnalysis2015⁶ to subtract background decay and obtain distance distributions using Tikhonov regularisation fitting. The appropriate background dimension was fitted and Tikhonov regularization parameter α was determined using L-curve fitting. Results are summarized in Table S1.

| Sample | $\langle r \rangle / \text{nm}$ | $\sigma(r) / \text{nm}$ | $\alpha =$ |
|---------------|---------------------------------|-------------------------|------------|
| NGB | 2.25 | 0.24 | 5 |
| Mb-S3R1 | 3.17 | 0.28 | 5 |
| Mb-S117R1 | 2.57 | 0.17 | 1 |
| Mb-S3R1S117R1 | 2.99 | 0.60 | 100 |
| S3R1-S117R1 | 3.67 | 0.81 | 1 |

Table S1: Table detailing the distances and their respective distances obtained using DeerAnalysis and the regularization parameter α used.

DEER data with rotamer simulation

Rotamer analysis was carried out for the Metmyoglobin mutants using MMM 2015⁷ and MtsslWizard⁸. The MMM simulations were carried out using a selection of custom libraries including: R1A UFF 216 298K, R1A UFF 216 CASD 298K and R1A Xray 298K. The MtsslWizard simulation was carried out using the loose Van der Waals approximation. A comparison of the measured distance distribution (black) and the distributions predicted by

MMM and MtsslWizard (colored) are shown in Figure S1 below along with the corresponding raw experimental data, background corrected data and the resulting Pake patterns obtained using DeerAnalysis 2015⁶.

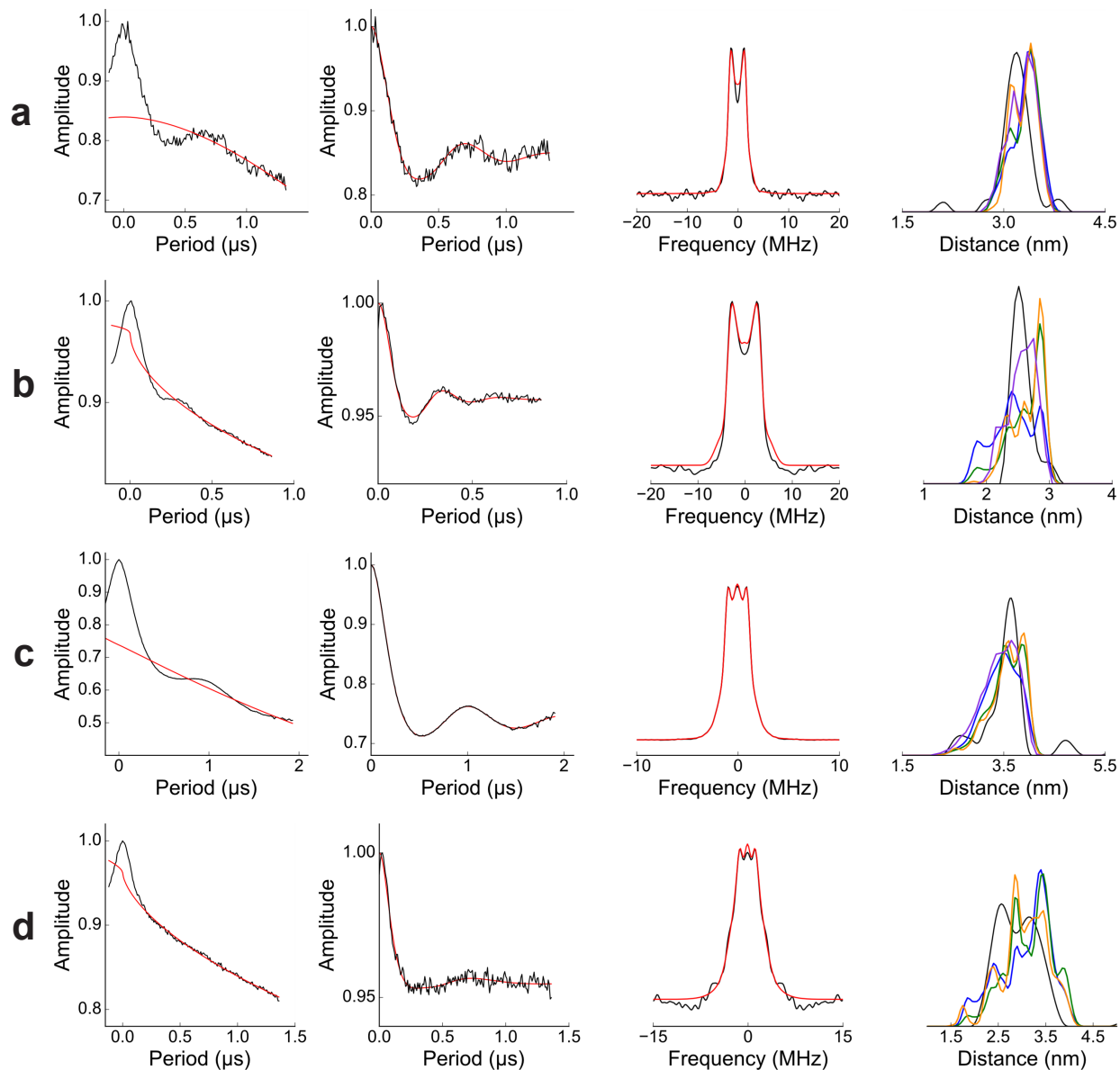


Figure S1: DEER data for all Metmyoglobin mutants and their comparisons with various rotamer library derived distance distribution simulations. (a) Mb-S3R1 at 6 K, (b) Mb-S117R1 at 6 K, (c) Mb-S3R1-S117R1 at 58 K and (d) Mb-S3R1-S117R1 at 6 K. Column 1 shows normalized experimental data with background fit in red, column 2 shows background corrected data (black) with red line showing the fit obtained using DeerAnalysis2015. column 3 shows the resulting Fourier transform of data in column 2 (Pake pattern) and column 4 showing the resulting distance distribution (black) using MMM libraries: R1A UFF 216 298K (blue), R1A UFF 216 CASD 298K (green) and R1A Xray 298K (orange), and MtsslWizard in purple.

For each of the mutants, the simulated distances were up to 0.3 nm different than experimentally measured at W-band. However, this is within the bounds of accuracy of the rotamer-library-based approach, although we also do not rule out contributions from freezing-induced changes to the spin label.

On the other hand we do not expect orientational effects to significantly affect the mean distance. Although the heme is expected to be relatively rigid, and the pump pulse will be highly selective, a broad range of Euler angles will still be excited by a probe pulse situated towards the center of the Fe spectrum. Similarly an even broader range of Euler angles is excited by the wideband pump pulse centred on the g_y part of nitroxide, which is also expected to have a rather broad range of orientations with respect to the heme. Thus a reasonable approximation to a full Pake pattern is expected. It should be noted that the maximum frequency offset between pump and probe is limited by the 800 MHz bandwidth of the 1 kW amplifier used on HiPER.

The spin density is also expected to be largely centred on the Fe, as nitrogen and proton hyperfine couplings are relatively small⁹.

T₁ measurements

Inversion recovery experiments were conducted both at W-band and Q-band (using a 150 W Bruker Elexsys E580 Q-band system) on the doubly labeled Mb-S3R1-S117R1 at the probe (Fe) position of the spectrum. The pulse sequence used was π -T- $\pi/2$ - τ - π - τ -*echo*. At W-band, τ was 276 ns, chosen to minimize ESEEM, and T was incremented from 50 ns in 100 ns steps for 601 steps, $\pi/2$ and π pulse lengths were 5 and 10 ns and the sequence repetition frequency was set to 100 Hz. In the Q-band experiments, τ was 312 ns, chosen to minimize ESEEM, T was incremented from 380 ns in 3000 ns steps for 1200 steps at 5, 6, 8 K, at 10 K it was incremented from 380 ns in 1000 ns steps for 600 steps, and at 15 K it was incremented in 100 ns steps for 600 steps. The $\pi/2$ and π pulse lengths were 16 and 32 ns and the sequence repetition frequency was set to 250 Hz. The W-band and Q-band curves are shown in Figure S2 (a) and (b), where it should be noted that sensitivity decreases rapidly with increasing temperature. The data was fitted using MatLAB curve fitting toolbox, to the equation $f(x) = c - a \cdot \exp(-b \cdot x)$ where $b = 1/T_1$. At 5 K the T₁ of the Mb is 30.8 μ s at W-band and 1.1 ms at Q-band. A shorter T₁ allows much faster averaging of data in DEER measurements at W-band.

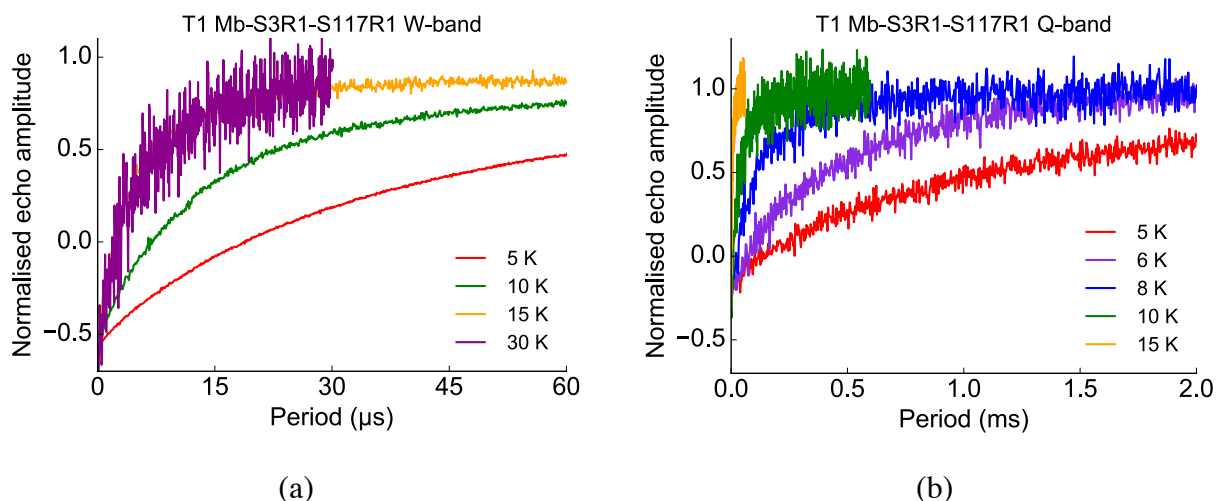


Figure S2: Inversion recovery T1 experiment results on Mb-S3R1-S117R1

Phase memory T_m measurements

Phase memory time experiments were conducted at W-band and Q-band on the doubly labeled Mb-S3R1-S117R1 at the probe (Fe(III)) position using the following sequence: $\pi/2$ -T- π -T-*echo*. At W-band this was carried out with $\pi/2$ and π pulses of 5 and 10 ns. T was incremented from 200 ns in 10 ns steps for 301 steps. This was carried out at 5, 15 and 25 K. At Q-band the pulse lengths were 16 and 32 ns, and T was incremented from 180 ns in 4 ns steps for 1024 steps. This was carried out at 5, 10 and 15 K. Results are shown in Figure S3.

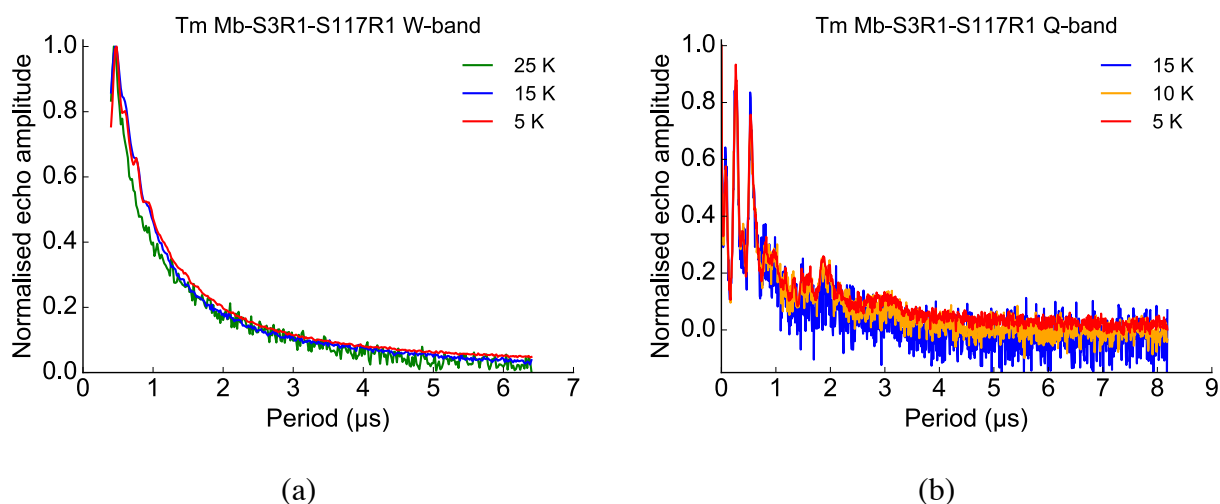


Figure S3: Phase memory time (T_m) experimental results at W-band (a) and Q-band (b).

As seen in Figure S3, both W-band and Q-band show strong ESEEM effects in the echo decay due to coupling of the Fe(III) to nitrogen and protons in the surrounding porphyrin ring. The effect is much more pronounced at Q-band than at W-band. The T_m at W-band at 5 K is approximately 1.1 μ s.

Composite pulses

Composite pulses consist of a number of sub pulses of varying phase that are usually designed to produce an overall 90° or 180° rotation of spin packets. They are described by the notation $(\beta_1^0)_{\phi_1} (\beta_2^0)_{\phi_2} \dots (\beta_n^0)_{\phi_n}$ where (β_p^0) describes the nominal flip angle (usually 90° or 180°) of the sub-pulse p , and ϕ_p describes its phase, or axis of rotation. The original 180° equivalent composite pulse, $90_{90}180_{90}90_{90}$ (Ref¹⁰) (when applied to a set of spins at equilibrium, $M_z // z$) thus equates to a 90° rotation around the y-axis ($\phi=90^\circ$), rotating the spins into the transverse plane along x, followed by a 180° rotation around this axis ($\phi=0^\circ$), finishing with another 90° rotation around the y-axis. The sequence is able to compensate for B_1 inhomogeneity by ‘helping’ or ‘hindering’ spins that under and over rotate due to spatial applied field inhomogeneity. The same argument applies for compensation for frequency offset between the resonance frequency of the spin and that of the pulse frequency. This manifests itself as an increase in effective flip angle of the spins, which can be considered as the rotation axis being tilted by an angle Δ towards +z. The $90_0 180_{180} 270_0$ composite π pulses used in this paper have the advantage they are relatively short sequences but increase bandwidth and compensate for applied field inhomogeneity to improve sensitivity.

Composite pulse sequences

Composite pulse combinations in the Neuroglobin study are detailed in Figure S4. Sequence A uses all standard π -pulses and is referred to as ‘normal’ in plots and text. In sequence B all π -pulses are replaced by composite pulses, and is referred to as ‘all composite.’ Sequence C uses a composite pump pulse and standard π -pulses in the probe sequence and is referred to as ‘pump.’ Sequence D uses composite probe π -pulses, and a standard pump pulse and is referred to as ‘probe.’

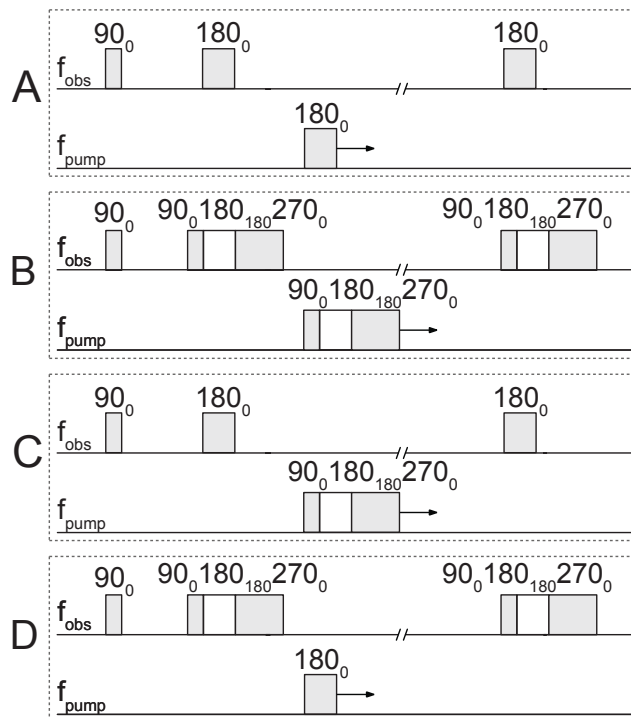


Figure S4: Diagram showing composite DEER sequences used in Figure 2. A- Normal, B- all composite, C- pump composite, D- probe composite.

Field swept echo and simulations

The W-band spectra shown in Figure 1 (main text) and in Figure S5 below was generated using the EasySpin package¹¹. Human neuroglobin was simulated using the g -values from Vinck et al, with $\mathbf{g}=(1.30,2.17,3.10)$ ¹². The g -values for sperm whale myoglobin were taken from Zhao et al, where $\mathbf{g}=(1.55,2.28,2.90)$ ¹³. The g -values show approximate agreement with the low spin peaks observed in cw spectra taken at X-band at 10 K (See Figure S6). The nitroxide label was simulated using typical g -values for experiments at this field, $\mathbf{g}=(2.0083,2.0063,2.0024)$. Figure S5 shows the field-swept echo spectra obtained for Mb-S117CR1 (inset) overlaid with the simulated spectra. Due to the limitation of the persistent magnet's sweep coil, it is only possible to view ± 200 mT around the center of field (shown inset) making it impossible to view the entire Fe(III) spectra at this frequency. Other Mb mutant spectra have been omitted due to similarity. The sharp equi-distant peaks (6-line pattern) observed in both plots, Figure 1 (main text) and Figure S5 are attributed to Mn(II) contaminants, which are observed at 6 K. They are not expected to effect the DEER measurements, as they are fast relaxing.

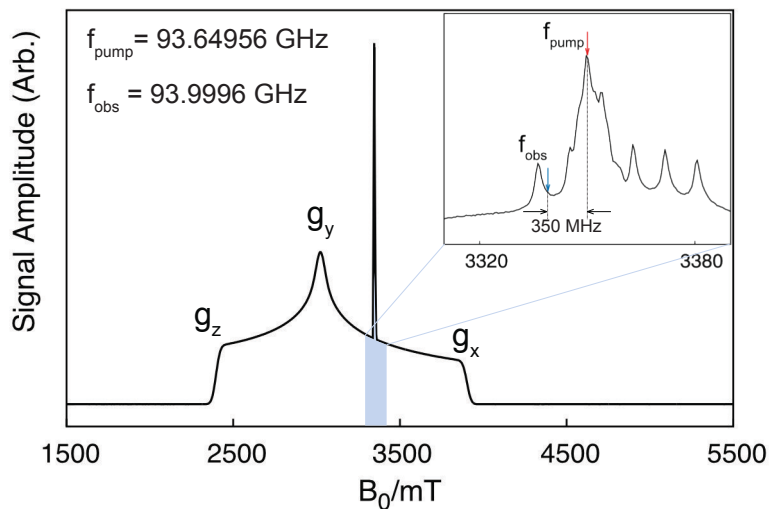


Figure S5 Mb-S117R1 field-swept echo experiment overlaid with simulation of the spectra generated using EasySpin¹¹ at 94 GHz. Blue shaded part indicates the part of spectrum that is viewed inset.

High-spin Fe(III) in Mb

The presence of high spin ($s=5/2$) and low spin ($s=1/2$) Fe(III) in the metmyoglobin mutants has been confirmed in a 10 K CW EPR spectrum that was taken at X-band with S3R1 imidazole-bound protein shown in Figure S6. This is shown through the presence of high spin ($s=5/2$) lines at $g=2$ and 6, as well as the low spin peaks around $g=2.28$ and 2.90 as predicted in Reference¹³. The peak at $g=1.55$ is out with the measured range.

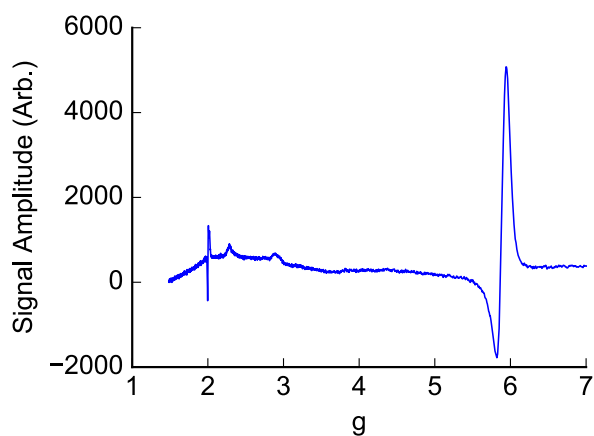


Figure S6: X-band cw spectra of Mb-S3R1 taken at 10 K.

The high spin Fe(III) is observed in low temperature pulsed experiments as a very fast relaxing distorted echo, which decays rapidly, and so is not present in the refocused DEER echo.

Signal to Noise Measurements

Signal to noise ratios were calculated by dividing the signal intensity (modulation depth) by the standard deviation of the noise. The noise was extracted from the raw DEER data by subtracting a smoothed version created from a suitable ‘moving average’, similar to the method reported by Goldfarb et al¹⁴.

Comparison with X-band DEER

DEER measurements have previously been made on NGB-C120R1 at X-band¹ where a signal to noise ratio of 21 was obtained after 24 hours of averaging at 15 K. In comparison the signal-to-noise ratios obtained at W-band using standard and composite-pulses, after 30 minutes averaging at 6 K are shown in Table S2.

| Sequence | SNR | Normalised ratio |
|-------------------|--------|------------------|
| Normal (A) | 42.40 | 1.00 |
| All-composite (B) | 128.73 | 3.03 |
| Pump (C) | 67.45 | 1.59 |
| Probe (D) | 75.52 | 1.78 |

Table S2: Comparison of the signal to noise for DEER composite sequences used on NGB-C120R1.

Allowing for the differences in averaging time, and an increase of ~ 1.3 in sample concentration at W-band, results in an overall sensitivity enhancement factor of 31, a factor of 3 of which can be directly attributed to the use of wideband composite pulses. It should also be noted that in the W-band measurement an averaging rate of 1 kHz was used, which was not fully optimized at that time.

Comparison with Q-band DEER

A direct sensitivity comparison between Q-band and W-band was made using the Mb-S117R1 system and is shown in Figure S7.

Q-band measurements were carried out on a Bruker Eleksys E580 system using a high power (150 W) TWT amplifier with a probe head supporting a cylindrical resonator ER 5106QT-2w that operates at a frequency around 34 GHz in the TE012 mode. The Q-band experiments were conducted at a temperature of 15 K (limited by T_1 relaxation time). The frequency of separation between pump and probe was 80 MHz (limited by the cavity).

Inter-pulse delays were $\tau_1=216$ ns and $\tau_2 = 1000$ ns, using observer pulse length of 32 ns and 26 ns for the pump pulse. The pump pulse was started 80 ns after the first π pulse on the observer sequence and was incremented in 8 ns steps for 132 steps. This was averaged at 3.3 kHz for 36 scans taking approximately 18 minutes to run. W-band measurements were made at 6 K using the previously described protocol, and averaged for the same time as the Q-band measurements.

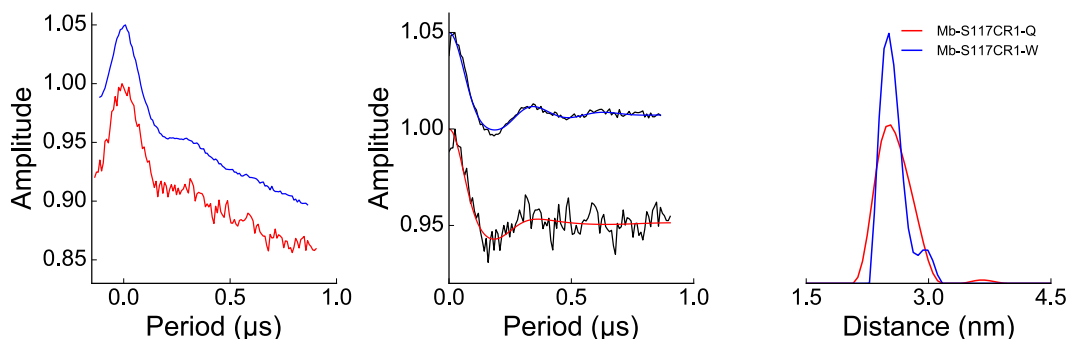


Figure S7 Comparison of W-band with composite pulses (blue) and Q-band (red) DEER traces obtained using sample Mb-S117CR1. Left shows raw normalized data, center shows data after background correction with fit added, and right shows the corresponding distance distributions.

The signal-to-noise ratios for Q-band and W-band (with composite pulses) were calculated to be 28 and 156 respectively. This equates to an improvement of 5.5 times in signal-to-noise. It should be noted that the HiPER sample holder can accommodate a large sample volume (80-150 μL , 90 μL in this case), in comparison with 50 μL used in the Q-band experiments.

References

- (1) Ezhevskaya, M.; Bordignon, E.; Polyhach, Y.; Moens, L.; Dewilde, S.; Jeschke, G.; Van Doorslaer, S. Distance Determination between Low-Spin Ferric Haem and Nitroxide Spin Label Using DEER: The Neuroglobin Case. *Mol. Phys.* **2013**, *111*, 2855–2864.
- (2) Neumann, H.; Hancock, S. M.; Buning, R.; Routh, A.; Chapman, L.; Somers, J.; Owen-Hughes, T.; van Noort, J.; Rhodes, D.; Chin, J. W. A Method for Genetically Installing Site-Specific Acetylation in Recombinant Histones Defines the Effects of H3 K56 Acetylation. *Mol. Cell* **2009**, *36*, 153–163.
- (3) Gasteiger, E.; Hoogland, C.; Gattiker, A.; Duvaud, S.; Wilkins, M. R.; Appel, R. D.; Bairoch, A. Protein Identification and Analysis Tools on the ExpASY Server. In *(In) John M. Walker (ed): The Proteomics Protocols Handbook, Humana Press (2005).*; Walker, J., Ed.; Humana Press: New York, NY, 2005.
- (4) Hanania, G. I.; Yeghiayan, A.; Cameron, B. F. Absorption Spectra of Sperm-Whale Ferrimyoglobin. *Biochem. J.* **1966**, *98*, 189–192.
- (5) Cruickshank, P. A. S.; Bolton, D. R.; Robertson, D. A.; Hunter, R. I.; Wylde, R. J.; Smith, G. M. A Kilowatt Pulsed 94 GHz Electron Paramagnetic Resonance Spectrometer with High Concentration Sensitivity, High Instantaneous Bandwidth, and Low Dead Time. *Rev. Sci. Instrum.* **2009**, *80*, 103102.
- (6) Jeschke, G.; Chechik, V.; Ionita, P.; Godt, A.; Zimmermann, H.; Banham, J.; Timmel, C. R.; Hilger, D.; Jung, H. DeerAnalysis2006—a Comprehensive Software Package for Analyzing Pulsed ELDOR Data. *Appl. Magn. Reson.* **2006**, *30*, 473–498.
- (7) Polyhach, Y.; Bordignon, E.; Jeschke, G. Rotamer Libraries of Spin Labelled Cysteines for Protein Studies. *Phys. Chem. Chem. Phys.* **2011**, *13*, 2356–2366.
- (8) Hagelueken, G.; Ward, R.; Naismith, J. H.; Schiemann, O. MtsslWizard: In Silico Spin-Labeling and Generation of Distance Distributions in PyMOL. *Appl. Magn. Reson.* **2012**, *42*, 377–391.
- (9) Vinck, E.; Van Doorslaer, S.; Dewilde, S.; Mitrikas, G.; Schweiger, A.; Moens, L. Analyzing Heme Proteins Using EPR Techniques: The Heme-Pocket Structure of Ferric Mouse Neuroglobin. *J. Biol. Inorg. Chem.* **2006**, *11*, 467–475.
- (10) Levitt, M. H.; Freeman, R. NMR Population Inversion Using a Composite Pulse. *J. Magn. Reson.* **1979**, *33*, 473–476.

- (11) Stoll, S.; Schweiger, A. EasySpin, a Comprehensive Software Package for Spectral Simulation and Analysis in EPR. *J. Magn. Reson.* **2006**, *178*, 42–55.
- (12) Vinck, E.; Van Doorslaer, S.; Dewilde, S.; Moens, L. Structural Change of the Heme Pocket due to Disulfide Bridge Formation Is Significantly Larger for Neuroglobin than for Cytochrome c. *J. Am. Chem. Soc.* **2004**, *126*, 4516–4517.
- (13) Zhou, Y.; Bowler, B. E.; Lynch, K.; Eaton, S. S.; Eaton, G. R. Interspin Distances in Spin-Labeled Metmyoglobin Variants Determined by Saturation Recovery EPR. *Biophys. J.* **2000**, *79*, 1039–1052.
- (14) Mentink-Vigier, F.; Collauto, A.; Feintuch, A.; Kaminker, I.; Tarle, V.; Goldfarb, D. Increasing Sensitivity of Pulse EPR Experiments Using Echo Train Detection Schemes. *J. Magn. Reson.* **2013**, *236*, 117–125.